Supporting Information

Aufderheide et al. 10.1073/pnas.1510449112

SI Materials and Methods

Protein Purification and Characterization. 26S proteasomes were purified as described previously (1). In brief, an affinity purification of 26S proteasomes via Rpn11-3FLAG from yeast cell lysate (YYS40: MATa *RPN11-3FLAG*::*HIS3*) was followed by further isolation using a sucrose gradient. To obtain an estimate of subunit abundances in the sample, we subjected the purified sample to mass spectrometry analysis and label-free quantification according to the intensity-based absolute quantification (iBAQ) value (2, 3). To determine the approximate amount of Ubp6 with respect to the canonical RP subunits, we computed the ratio of the Ubp6 iBAQ value and the average iBAQ value of the RP subunits.

GST-Ubp6 (pDL74) (4) was expressed in *Escherichia coli* and purified essentially as described in ref. 4. To verify catalytic activity of the recombinant protein, we performed hydrolysis assays of fluorescent ubiquitin–7-amido-4-methylcoumarin (Ub–AMC) (Boston Biochem) in the absence and presence of purified 26S proteasomes. Before the enzymatic reaction was started, the sample was incubated on ice for 15 min. Ub–AMC (40 nM) hydrolysis was measured at 360 nm excitation/465 nm emission using a GENios Pro (TECAN) fluorometer.

Additional hydrolysis assays of the 26S proteasomes in the presence of Ubp6 and/or UbAld were performed using GGL-AMC (Bachem) as a substrate. First, 26S proteasomes were incubated with Ubp6 for 15 min on ice. UbAld was added, followed by further incubation for 15 min on ice. The catalytic reaction was started by adding the GGL-AMC peptide (40 nM) and was monitored with the setup used for Ub-AMC.

To confirm the interaction between GST-Ubp6 and UbAld (Boston Biochem), a pulldown assay was performed against the Rpn11-3XFlag tag using M2 beads (Sigma). The samples were further subjected to SDS/PAGE analysis. Gels were analyzed by Coomassie staining or immunoblotting.

Cryo-EM and Image Analysis. To study the structure of the 26S–Ubp6 complex, datasets of the three samples, 26S–Ubp6 (300 nM 26S, 3 μM Ubp6), 26S–Ubp6–UbAld (300 nM 26S, 3 μM Ubp6, 12 μM UbAld), and 26S–UbAld (300 nM 26S, 12 μM UbAld) were collected on a Titan Krios with a Falcon II camera using the FEI EPU software. Images were acquired at a pixel size of 1.4 Å at the specimen level, a total dose of 45 electrons distributed over seven frames, and with a nominal defocus varying between 2 and 3 μm. The frames were translationally aligned and averaged using the algorithm from ref. 5. Double-capped 26S proteasome particles were automatically localized as described in ref. 6. Low-quality particles were filtered out (cleaning) using RELION 2D classification (7). The resulting particles were reconstructed and classified in an in-house modified version of XMIPP, which allows us to restrict the in-plane rotation and to focus the analysis on one of the RPs (8). Additional classification using a small mask was performed as described in ref. 9. The mask was chosen to focus on the area between Rpn1 and Rpn10, where the larger part of the extra density in the 26S–Ubp6–UbAld reconstruction is located.

For comparison of the state occupancies, subsets of equal size (~180,000 particles) were classified into six classes. The number of classes was chosen according to the dataset size and oversampling of the number of expected conformations, to be sensitive to less occupied states. The resulting densities then were compared with the known conformations s1, s2, and s3 by cross-correlation and were grouped accordingly.

High-resolution refinement was performed using two separate halves of the data (gold-standard) as described in ref. 8. The overall resolution was determined according to ref. 7, and the local resolution was computed using Bsoft (10), and the map was filtered accordingly.

Fitting. To position the catalytic USP domain of Ubp6 into the EM density, densities were simulated from the $Ubp6^{104-499}$ crystal structure (PDB ID code 1VJV) and from a $Ubp6^{104-499}$–UbAld model. The latter was constructed by superposing the $Ubp6^{104-499}$ crystal structure onto Usp14 in the Usp14–UbAld crystal structure (PDB ID code 2AYO) (11). Both the simulated and the experimental density were filtered to 15 Å, which is the approximate resolution in the respective area of the 26S–Ubp6–UbAld map.

To determine the approximate starting position and orientation, a template-matching procedure was performed, using pyTom (12), and the template volume was aligned according to the correlation peak (Fig. S7*A*). Starting from this position, a six-dimensional correlation scan (exhaustive translation and orientation search) of the simulated density with the area around the extra density was performed using the TOM package (13). For statistical evaluation, Z-scores were calculated from the cross-correlation values in a two-step procedure. First, a Fisher transformation was applied to the data; then the resulting values were normalized by subtracting the mean and dividing by the SD. The results were depicted against the angular distance from the starting position. To evaluate the specificity of the fit, searches on the two independent gold-standard reconstructions and on a decoy volume of equal size, which was randomly extracted from the region of the 20S core particle, were performed (Fig. S7 *B* and *C*).

XL-MS. XL-MS was carried out essentially as described previously (14). In short, roughly 40 μg of sample was cross-linked directly with 1 mM disuccinimidyl suberate d0/d12 (DSS; Creativemolecules Inc.), digested with trypsin, and subsequently enriched for cross-linked peptides. LC-MS/MS analysis was carried out on an Orbitrap Elite mass spectrometer (Thermo Electron). Data were searched using xQuest in iontag mode against a database containing GST-Ubp6, UbAld, and all subunits of the 26S proteasome in *S. cerevisiae* with a precursor mass tolerance of 10 ppm. For matching of fragment ions, tolerances of 0.2 Da for common ions and 0.3 Da for cross-link ions were used. Potential cross-links were validated statistically from fragment ion spectra, and false-discovery rates (FDRs) were assigned using xProphet (15). Only unique cross-links were considered, and only high-confidence cross-linked peptides that were identified with a delta score (ΔS) below 0.8 and an Id score above 27 were selected for this study, corresponding to an FDR of <0.13. Spectra of potential cross-links also were analyzed by visual inspection to ensure good matches of ion series on both cross-linked peptide chains for the most abundant peaks.

1. Sakata E, et al. (2011) The catalytic activity of Ubp6 enhances maturation of the proteasomal regulatory particle. *Mol Cell* 42(5):637–649.
2. Cox J, et al. (2014) Accurate proteome-wide label-free quantification by delayed normalization and maximal peptide ratio extraction, termed MaxLFQ. *Mol Cell Proteomics* 13(9):2513–2526.
3. Steen H, Mann M (2004) The ABC's (and XYZ's) of peptide sequencing. *Nat Rev Mol Cell Biol* 5(9):699–711.
4. Leggett DS, et al. (2002) Multiple associated proteins regulate proteasome structure and function. *Mol Cell* 10(3):495–507.

5. Li X, et al. (2013) Electron counting and beam-induced motion correction enable near-atomic-resolution single-particle cryo-EM. *Nat Methods* 10(6):584–590.
6. Beck F, et al. (2012) Near-atomic resolution structural model of the yeast 26S proteasome. *Proc Natl Acad Sci USA* 109(37):14870–14875.
7. Scheres SH (2012) RELION: Implementation of a Bayesian approach to cryo-EM structure determination. *J Struct Biol* 180(3):519–530.
8. Unverdorben P, et al. (2014) Deep classification of a large cryo-EM dataset defines the conformational landscape of the 26S proteasome. *Proc Natl Acad Sci USA* 111(15):5544–5549.
9. Bohn S, et al. (2010) Structure of the 26S proteasome from Schizosaccharomyces pombe at subnanometer resolution. *Proc Natl Acad Sci USA* 107(49):20992–20997.
10. Cardone G, Heymann JB, Steven AC (2013) One number does not fit all: Mapping local variations in resolution in cryo-EM reconstructions. *J Struct Biol* 184(2):226–236.
11. Hu M, et al. (2005) Structure and mechanisms of the proteasome-associated deubiquitinating enzyme USP14. *EMBO J* 24(21):3747–3756.
12. Hrabe T, et al. (2012) PyTom: A python-based toolbox for localization of macromolecules in cryo-electron tomograms and subtomogram analysis. *J Struct Biol* 178(2):177–188.
13. Nickell S, et al. (2005) TOM software toolbox: Acquisition and analysis for electron tomography. *J Struct Biol* 149(3):227–234.
14. Leitner A, Walzthoeni T, Aebersold R (2014) Lysine-specific chemical cross-linking of protein complexes and identification of cross-linking sites using LC-MS/MS and the xQuest/xProphet software pipeline. *Nat Protoc* 9(1):120–137.
15. Walzthoeni T, et al. (2012) False discovery rate estimation for cross-linked peptides identified by mass spectrometry. *Nat Methods* 9(9):901–903.

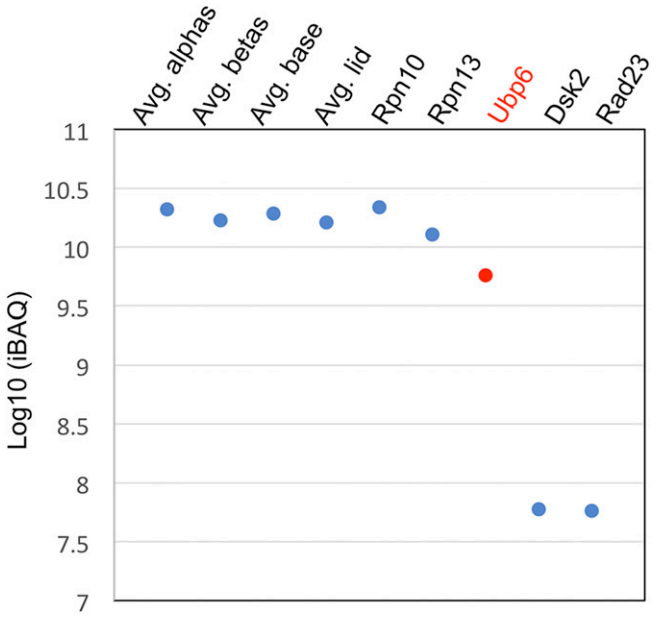

Fig. S1. Subunit abundance of the purified 26S proteasomes was analyzed by intensity-based absolute quantification (iBAQ). Comparison of iBAQ values suggested a stoichiometry of approximately 30% of Ubp6 in the sample.

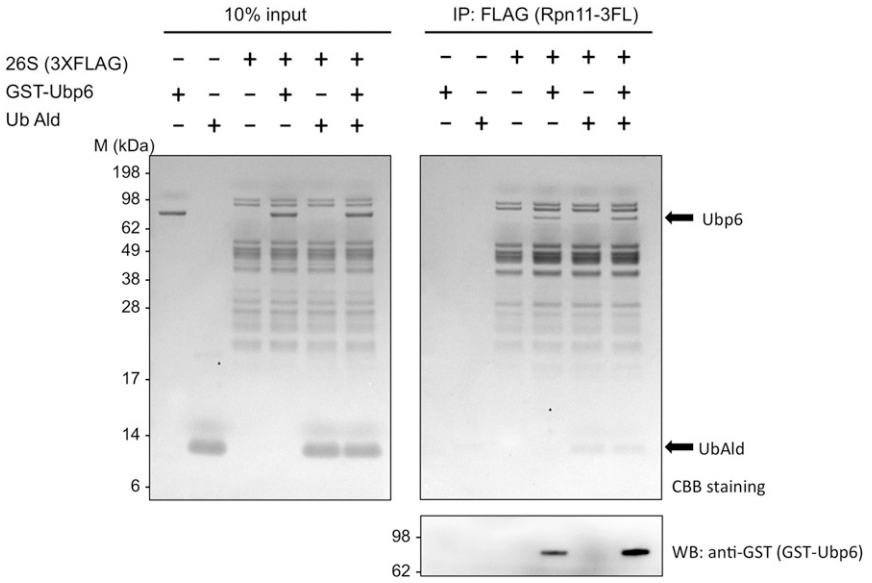

Fig. S2. Purified GST-Ubp6 binds to the 26S proteasome. A pulldown assay was performed in the presence and absence of UbAld. The presence of UbAld slightly increases the interaction of Ubp6 with the 26S proteasome.

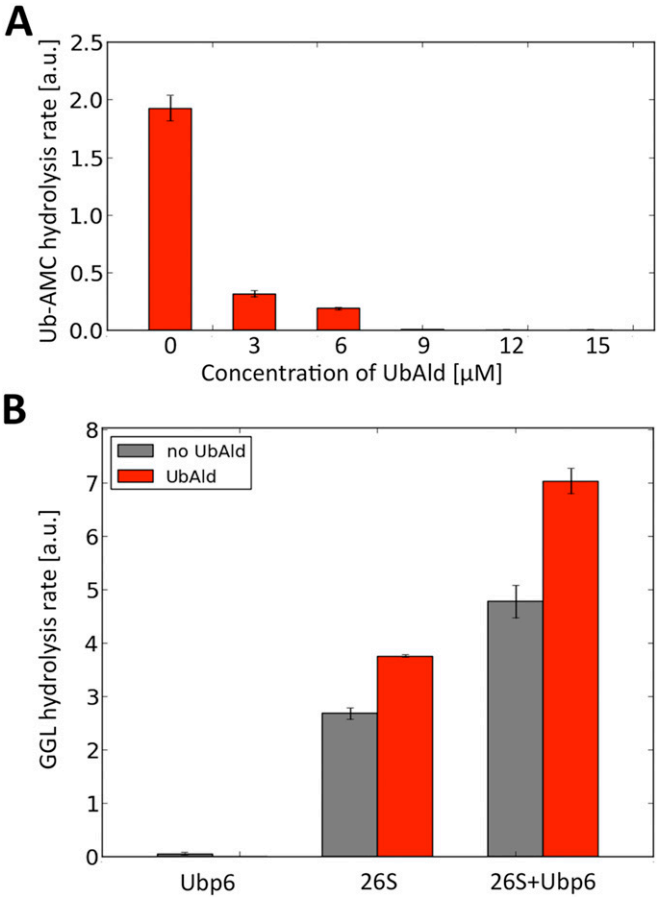

Fig. S3. (*A*) Ub-AMC hydrolysis rate of 26S–Ubp6 samples decreases with increasing concentration of UbAld, confirming its inhibitory effect on Ubp6. (*B*) Ubp6 (3 μM), WT 26S (10 nM), and WT 26S together with Ubp6 (10 nM and 3 μM, respectively) were tested for the activity of the 20S CP in the absence (gray) and presence (red) of UbAld (15 μM). The GGL-AMC hydrolysis rates indicate an activation of WT 26S proteasomes in the presence of Ubp6 as well as UbAld and qualitatively reproduce the results from ref. 1.

1. Peth A, Besche HC, Goldberg AL (2009) Ubiquitinated proteins activate the proteasome by binding to Usp14/Ubp6, which causes 20S gate opening. *Mol Cell* 36(5):794–804.

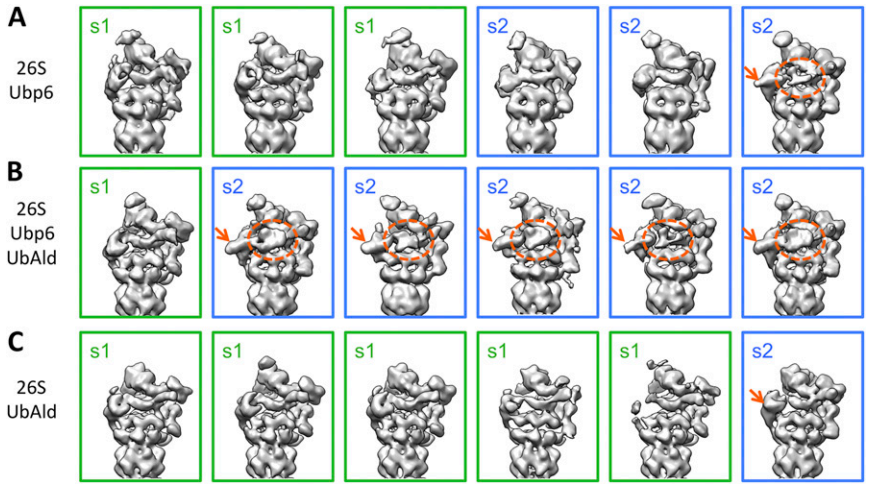

Fig. S4. 3D classification of 26S–Ubp6, 26S–Ubp6–UbAld, and 26S–UbAld. Subsets of equal size (~180,000 particles) were classified into six classes for26S–Ubp6 (*A*), 26S–Ubp6–UbAld (*B*), and 26S–UbAld (*C*). The classes were assigned to s1-like (green boxes) and s2-like (blue boxes) conformations through a cross-correlation analysis. For 26S–Ubp6–UbAld all s2-like classes show clear extra densities (orange ellipses and arrows), whereas for 26S–Ubp6 and 26S–UbAld only one class each includes indications of density in the respective area.

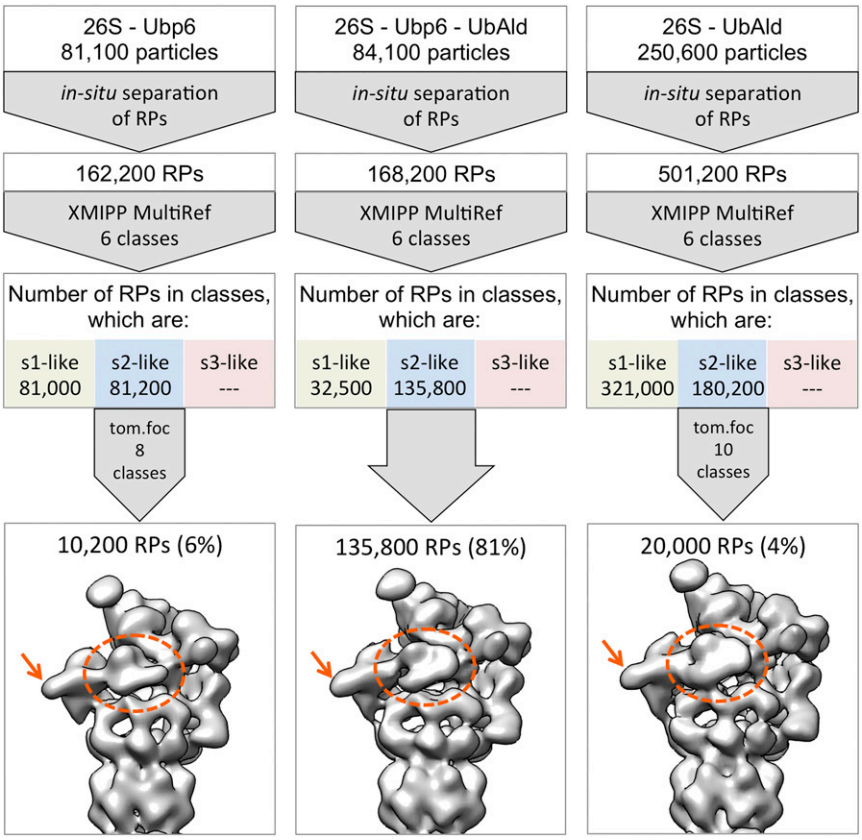

Fig. S5. Classification workflow to identify RPs exhibiting extra density in 26S–Ubp6, 26S–Ubp6–UbAld, and 26S–UbAld datasets. Steps of the 3D classification procedures applied to 26S–Ubp6 (*Left*), 26S–Ubp6–UbAld (*Center*), and 26S–UbAld (*Right*) datasets and according particle/RP numbers. "MultiRef" stands for multireference alignment using random seeds (here, six) as initial models; "tom.foc" is a correlation-based classification method implemented in the TOM package, here focused on the area of the extra density. Orange ellipses and arrows mark the extra densities in the final reconstructions of the classification results. Note the difference in the shape of the extra density in the 26S–Ubp6 reconstruction as compared with the other two.

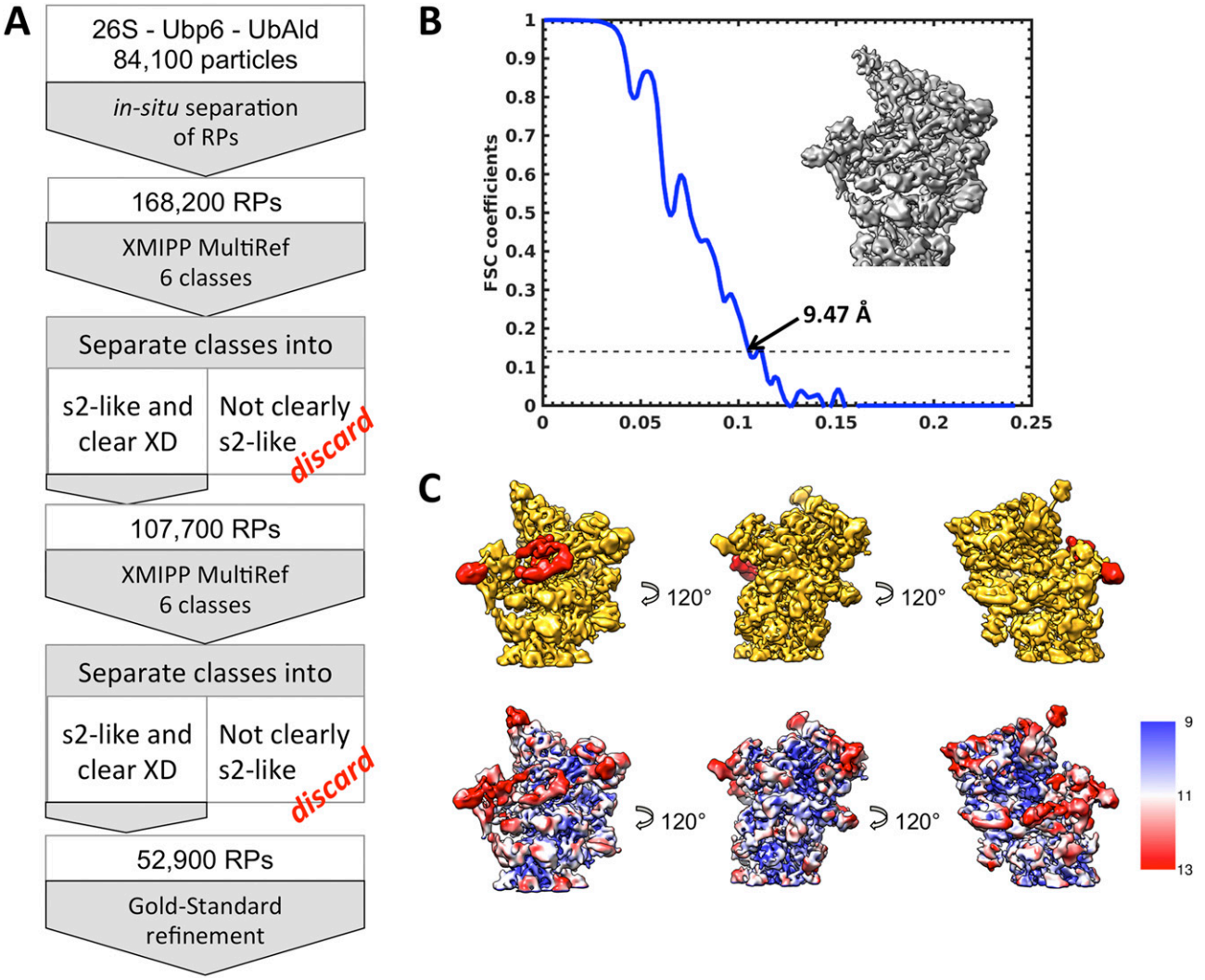

Fig. S6. High-resolution refinement of 26S–Ubp6–UbAld. (*A*) Workflow for cleaning the 26S–Ubp6–UbAld dataset before gold-standard refinement. (*B*) FSC curve of the refined structure (shown in the *Inset*) demonstrating the overall resolution of 9.5 Å. (*C*) Refined structure filtered according to the local resolution. (*Upper Row*) Localization of Ubp6 (shown in red). (*Lower Row*) Filtered map colored according to the local resolution. Although most of the integral parts of the 26S are at subnanometer resolution, the extra density is resolved to ∼14 Å.

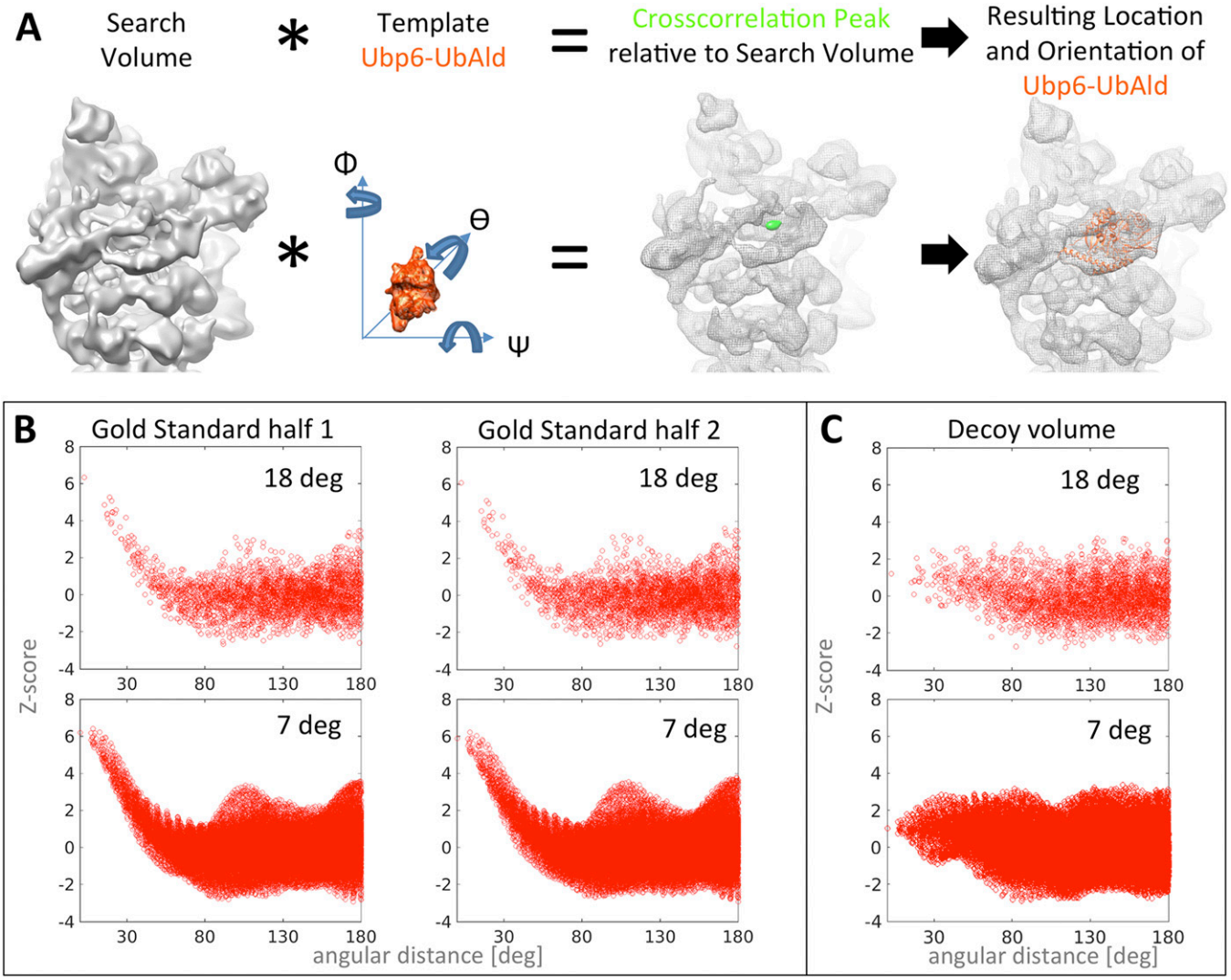

Fig. S7. Fitting of the Ubp6$^{104-499}$–UbAld model into the extra density. (*A*) Template-matching procedure to identify the approximate position and orientation of Ubp6 used as a starting position for the fits. (*B* and *C*) Z-scores for different fitting scenarios of simulated Ubp6$^{104-499}$–UbAld densities into the extra density of 26S–Ubp6–UbAld. To verify our fitting strategy, different scenarios were evaluated at different angular samplings (*Upper Rows*: 18°; *Lower Rows*: 7°). Identified maxima for different samplings are in good accordance for all scenarios. (*B*) Positioning was evaluated for the two gold-standard volumes separately, leading to highly consistent results. (*C*) As a further control, a decoy volume was randomly extracted from the region of the 20S core particle. Correlation between the simulated Ubp6$^{104-499}$–UbAld density and the decoy led to overall lower scores without any clear maximum.

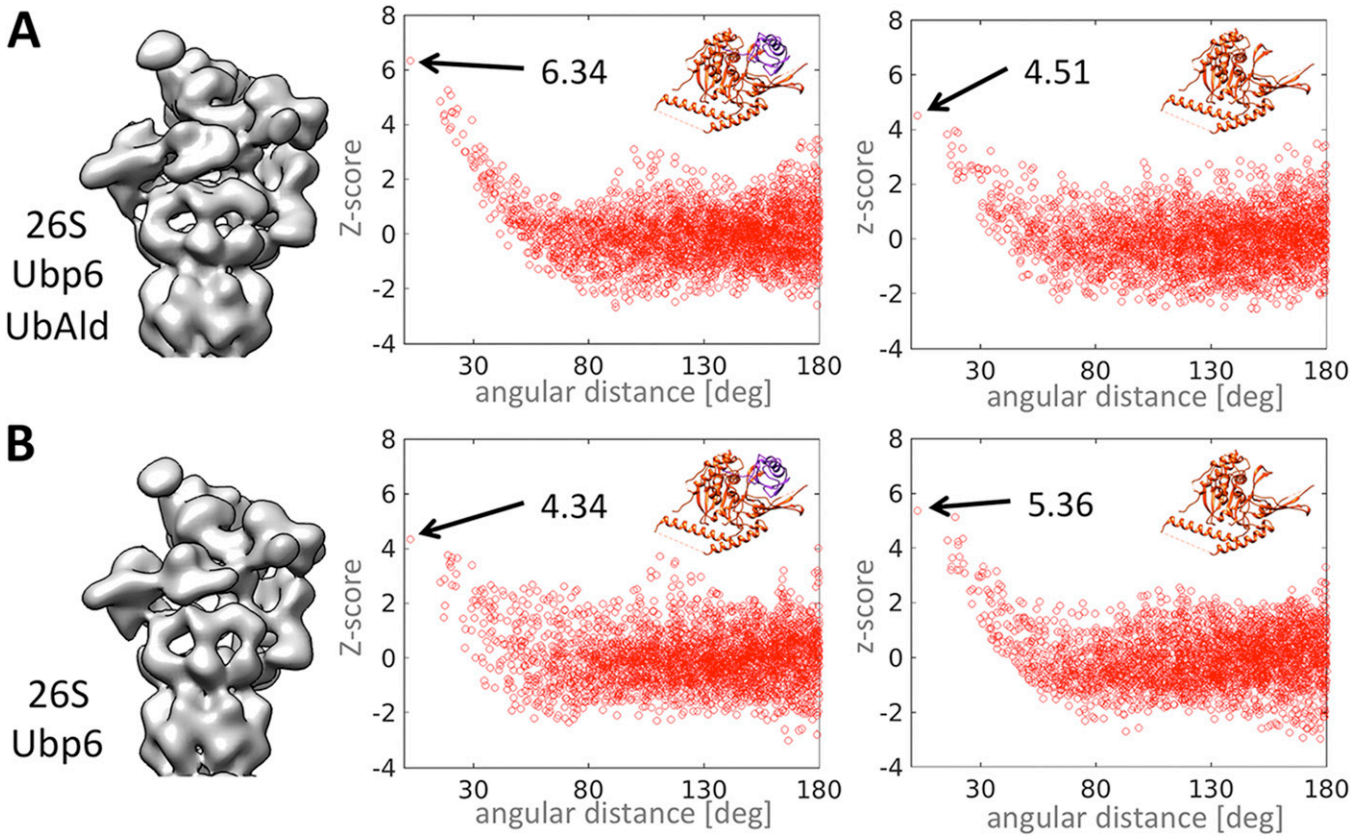

Fig. S8. Localization of UbAld. Fit results (Z-score) for extra densities of 26S–Ubp6–UbAld (*A*) and 26S–Ubp6 (*B*). Both maps were fitted with the models of Ubp6$^{104-499}$–UbAld (*Left*) and Ubp6$^{104-499}$ alone (*Right*). For 26S–Ubp6–UbAld the model containing UbAld led to higher Z-scores, whereas for 26S–Ubp6 the model without UbAld yielded better results. However, the position of the maximum remains the same.

Table S1. Cross-links between Ubp6 and integral subunits of the 26S proteasome identified by XL-MS

Cross-linked peptide	Protein1	Protein2	Type	AbsPos1	AbsPos2	ΔS	Id score	FDR
SFKSVLPIVLLNTLR-GSNQKPK-a3-b5	GST_Ubp6	sp|P40327|PRS4_YEAST	Interlink	177	20	0.6	31.57	0.045
SFKSVLPIVLLNTLR-YEPPVQSKFGR-a3-b8	GST_Ubp6	sp|P40327|PRS4_YEAST	Interlink	177	30	0.41	30.29	0.059
RKFDPSSSENVMTPR-IKIAHGTTTLAFR-a2-b2	GST_Ubp6	sp|P30656|PSB5_YEAST	Interlink	378	71	0.57	29.27	0.084
EIKRR-IHSKSMSVER-a3-b4	GST_Ubp6	sp|P33299|PRS7_YEAST	Interlink	375	394	0.63	28.52	0.112
EKNEKER-IHSKSMSVER-a5-b4	GST_Ubp6	sp|P33299|PRS7_YEAST	Interlink	370	394	0.73	28.14	0.112
RKFDPSSSENVMTPR-IHSKSMSVER-a2-b4	GST_Ubp6	sp|P33299|PRS7_YEAST	Interlink	378	394	0.38	27.07	0.126

Shown are the exact amino acid sequence of the cross-linked peptides and the position of the cross-linked lysine residue (cross-linked peptide); the name of the respective protein (protein1 and protein2), the nature of the cross-link (type); the absolute position of the cross-linked lysine residues within the UniProt or construct sequence (AbsPos1 and AbsPos2); the delta score of the respective crosslink (ΔS), which is a measure for how close the best assigned hit was scored in regard to the second best hit; the weighted sum of different scores used to assess the quality of the composite MS2 spectrum as calculated by xQuest (Id score); and the FDR as calculated by xProphet. All but the fifth cross-link involved disordered segments. Note: The residue numbers of GST_Ubp6 were chosen to have the first residue of Ubp6 numbered as 1, and residues of the GST-tag have negative values.